NUMERICAL ANALYSIS OF A NEAR-TO-REAL SCALE IN-SITU EXPERIMENT OF A DEEP GEOLOGICAL REPOSITORY

F. Dupray
Soil Mechanics Laboratory (LMS), School of Architecture, Civil and Environmental Engineering (ENAC), Ecole Polytechnique Fédérale de Lausanne (EPFL), Switzerland

B. François
Building, Architecture & Town Planning Department (BATir), Université Libre de Bruxelles, Belgium

L. Laloui
Soil Mechanics Laboratory (LMS), School of Architecture, Civil and Environmental Engineering (ENAC), Ecole Polytechnique Fédérale de Lausanne (EPFL), Switzerland

ABSTRACT: *Deep geological repository involving a multi-barrier system constitutes one of the most promising options to isolate high-level radioactive waste from the human environment. In order to certify the efficiency of waste isolation, it is essential to understand the behaviour of the confining geomaterials under a variety of environmental conditions. The efficiency of Engineered Barrier Systems (EBS) is highly based on the complex behaviour of bentonite. To improve the understanding of the processes involved in the EBS, results from a near-to-real scale experiment, the FEBEX experiment, are studied by means of a thermo-hydro-mechanical (THM) finite element approach including a consistent thermo-plastic constitutive model for unsaturated soils. The model also features a coupled THM approach of the water retention curve. The extended literature available on the behaviour of the FEBEX bentonite is used to calibrate the parameters. The results of the numerical simulations are compared with sensor measurements and show the ability of the model to reproduce the main features of the mechanical behaviour of the system. The hydraulic and thermal response is also realistically described by the model. The link between the confined swelling behaviour as tested in laboratory and the results of the real-scale experiment is clearly established by this simulation.*

1 INTRODUCTION

Over the coming years, definitive solutions will likely be available for the management of large quantities of high-level radioactive waste that mainly stem from the production of nuclear electricity. Deep geological repositories constitute one of the most promising options for isolating such waste from the human environment. In this context, the highly coupled thermo-hydro-mechanical (THM) phenomena that occur in engineered and geological barriers must be captured adequately by means of numerical analysis (Laloui et al., 2008). To validate and calibrate the mathematical models, numerical simulations of in-situ experiments reproducing comparable studies have to be performed. In such a way, the results of the experiment may be interpreted within the constitutive framework of the chosen models which in turn may improve the understanding of the phenomena involved.

The FEBEX (Full-scale Engineered Barriers EXperiment in crystalline host rock) in-situ test is a near-to-real experiment carried out in the underground laboratory at Grimsel (Switzerland). It uses the Spanish disposal concept for underground nuclear waste storage in granitic formations as its reference. The gallery, excavated in the granitic rock of the Aare Massif in central Switzerland, has a diameter of 2.28 m and a length of 71.4 m. Two heaters (0.95 m in diameter and 4.54 m long, the same dimensions as the canisters of the reference

disposal concept) were placed in the axis of the gallery at a 1 m distance from each other. The free space between the heaters and the granite was filled with compacted bentonite blocks for the last 17 m of the gallery. The 17 m long test zone was sealed by a concrete plug (Figure 1) (Lloret et al., 2004). During this in-situ experiment direct measurements, in terms of temperature, fluid pressure, humidity, total stresses and deformation of the confining structure, provided worthwhile information for the verification and the validation of mathematical models aimed at predicting the coupled THM processes occurring in such disposal. Several numerical predictions, or validations, have already been reported in the literature by Gens et al. (1998) and Alonso et al. (2005), among others. Gens et al. (2009) recently published a comprehensive paper on this in-situ heating test including observations, numerical analysis and interpretation. Experimental aspects considering the system of sensors were especially detailed in this paper and will not be further reviewed here. The present study brings additional information on various aspects of the problem, in particular the role of the irreversible straining of the bentonite, related to its thermo-plasticity and suction-induced hardening, is highlighted. In the present paper, the use of a constitutive model that considers the thermal and suction plasticities in a unique theoretical framework offers a unified constitutive approach for the modelling of the bentonite response. By doing so, the focus is made on the various thermo-hydro-mechanical couplings including important plastic mechanisms in the behaviour of bentonite.

Predictions of the THM behaviour of compacted bentonite and host rock have been performed by means of finite element simulations. These numerical analyses provide accurate information on the mechanical effects of temperature and suction evolution in the confining materials. To carry out the numerical analysis, the ACMEG-TS elasto-thermoplastic constitutive model for unsaturated soils (François & Laloui, 2008) has been implemented in the finite element code LAGAMINE (Charlier et al., 2001; Collin et al., 2002).

First, the paper presents a brief summary of the capabilities of the constitutive model and numerical tools used. Then, calibration and features of the numerical analysis performed are presented. Finally, the comparison between the results obtained and in-situ measurements is discussed, in terms of irreversible strains, coupling between mechanical, thermal and water retention responses and diffusion processes.

2 THEORETICAL APPROACH

The ACMEG-TS model (Advanced Constitutive Model in Environmental Geomechanics – Thermal and Suction effects) considers the material as a composition of a solid matrix and two species, in that case water and air. In order to uniquely describe the state of the material, four primary state variables are needed: gas pressure p_g, water pressure p_w, temperature T and solid displacement vector $\mathbf{u}$. The solid phase component is assumed to be incompressible, whereas the liquid phase is slightly compressible. The kinematics of fluid diffusion being slow with respect to thermal diffusion, the solid, liquid and gas phases are assumed to be in thermal equilibrium.

The model therefore uses three phases and models the three thermal, hydraulic and mechanical processes in a coupled way. Mass balances equations are written for the species rather than for the phases. The equilibrium equations, as well as water and heat flows, are described in a Lagrangian actualised formulation. Further details on these aspects can be found in other studies (Collin et al., 2002; Collin, 2003)

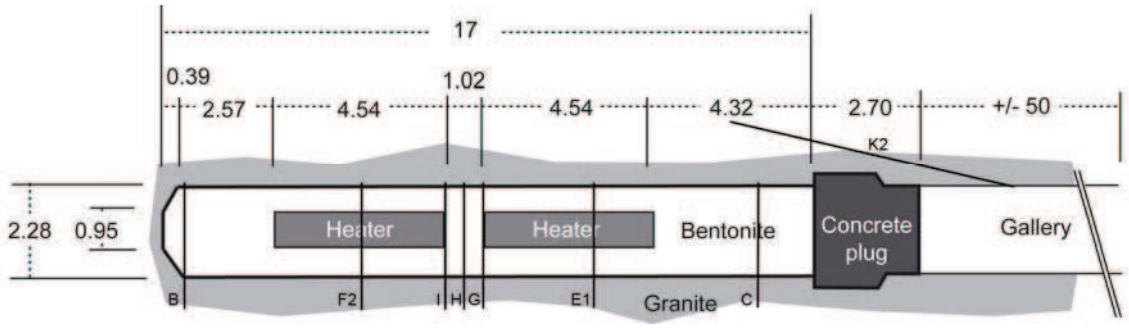

Figure 1: Layout of the FEBEX in-situ test, with localisation of the sections and boreholes (adapted from Gens *et al.* (2009)). Lengths in meters.

THM field equations

The mass conservation equations for the water and gas species are, respectively:

$$\underbrace{\frac{\partial}{\partial t}\left(\rho_w n S_r\right)+div\left(\rho_w \mathbf{f_l}\right)-Q_w}_{\text{Liquid water}}+\underbrace{\frac{\partial}{\partial t}\left(\rho_v n\left(1-S_r\right)\right)+div\left(\mathbf{i_v}+\rho_v \mathbf{f_g}\right)-Q_v}_{\text{Water vapour}}=0 \tag{1}$$

$$\underbrace{\frac{\partial}{\partial t}\left(\rho_a n\left(1-S_r\right)\right)+div\left(\rho_a \mathbf{f_g}+\mathbf{i_a}\right)-Q_a}_{\text{Dry air in gas phase}}+\underbrace{\frac{\partial}{\partial t}\left(\rho_a H_s n S_r\right)+div\left(\rho_a H_s \mathbf{f_l}\right)-Q_{da}}_{\text{Dissolved air in water}}=0 \tag{2}$$

where ρ_w, ρ_v and ρ_a are the bulk density of liquid water, water vapour, and dry air. $\mathbf{f_l}$ and $\mathbf{f_g}$ are the macroscopic velocity of the liquid and gas phases, respectively. $\mathbf{i_v}$ and $\mathbf{i_a}$ are the non-advective flux of water vapour and dry air. S_r is the degree of saturation. The Henry's coefficient, H_s, defining the proportion of dissolved air in the liquid phase, is taken to be equal to 0.017. Q_w, Q_v, Q_a and Q_{da} are volume sources of liquid water, water vapour, dry air and dissolved air in water, respectively.

The energy balance equation of the mixture has the following form:

$$\underbrace{\frac{\partial S_T}{\partial t}+L\frac{\partial}{\partial t}\left(\rho_v n\left(1-S_r\right)\right)}_{\text{Heat storage}}+\underbrace{div\left(\mathbf{f_T}\right)+L\cdot div\left(\mathbf{i_v}+\rho_v \mathbf{f_g}\right)}_{\text{Heat transfer}}-Q_T=0 \tag{3}$$

where $\mathbf{f_T}$ is the heat flow and Q_T is a volume heat source. L is the latent heat of water vaporisation. The enthalpy of the system S_T is given by:

$$S_T=\rho C_p\left(T-T_0\right) \tag{4}$$

where ρ and C_p are the density and the specific heat of the mixture (solid matrix with voids filled by gas and liquid), respectively. Those parameters are deduced from the properties of each phase:

$$\rho C_p=nS_r\rho_w c_{p,w}+\left(1-n\right)\rho_s c_{p,s}+n\left(1-S_r\right)\rho_a c_{p,a}+n\left(1-S_r\right)\rho_v c_{p,v} \tag{5}$$

where ρ_s is the soil grain bulk density and $c_{p,w}$, $c_{p,s}$, $c_{p,a}$ and $c_{p,v}$ are the specific heat of liquid water, solid, dry air and water vapour, respectively.

The soil equilibrium equation is given by:

$$div(\boldsymbol{\sigma}) + \mathbf{b} = 0 \tag{6}$$

where $\boldsymbol{\sigma}$ is the total (Cauchy) stress tensor, with compressive stress taken as positive and $\mathbf{b}$ is the body force vector which is equal to $\rho\mathbf{g}$ if the only body force is gravity.

3 ACMEG-TS: A SOIL CONSTITUTIVE MODEL

The behaviour of the solid matrix is assumed to be governed by the generalized effective stress tensor $\boldsymbol{\sigma}'$ through combinations of mechanical stresses and fluid pressures (Schrefler, 1984; Nuth & Laloui, 2008):

$$\boldsymbol{\sigma}' = \boldsymbol{\sigma} - p_g \mathbf{I} + S_r \left(p_g - p_w \right) \mathbf{I} \tag{7}$$

The term $(\boldsymbol{\sigma} - p_g \mathbf{I})$ is called the net stress, while $\left(p_g - p_w \right)$ is the matrix suction.

Mechanical behaviour

The mechanical model (François & Laloui, 2008), is based on an elasto-plastic framework, the total strain increment $d\boldsymbol{\varepsilon}$ being decomposed into non-linear, thermo-elastic, $d\boldsymbol{\varepsilon}^{\mathbf{e}}$ and plastic, $d\boldsymbol{\varepsilon}^{\mathbf{p}}$, components. The elastic part of the deformation is expressed as follows:

$$d\boldsymbol{\varepsilon}^{\mathbf{e}} = \mathbf{E}^{-1} d\boldsymbol{\sigma}' - \boldsymbol{\beta}_{\mathbf{T}} dT \tag{8}$$

The first term of Equation (8) is the contribution of the effective stress increment $d\boldsymbol{\sigma}'$ to the total elastic strain increment, through the non-linear elastic tensor $\mathbf{E}$. This tensor depends on the effective pressure. According to Equation (7), this part may follow from total stress or fluid pressure variations. The second term of Equation (8) is related to the thermo-elastic strain of the material, through the thermal expansion coefficient matrix, $\boldsymbol{\beta}_{\mathbf{T}} = (1/3)\beta_s' \mathbf{I}$.

The plastic mechanism of the material is induced by two coupled hardening processes: an isotropic and a deviatoric one. Using the concept of multi-mechanism plasticity, both mechanisms may induce volumetric plastic strain (Hujeux, 1979). Therefore the total volumetric plastic strain rate $d\varepsilon_v^p$ is the coupling variable linking the two hardening processes. The yield functions of the two mechanical plastic mechanisms have the following expressions (see Figure 2):

$$f_{iso} = p' - p_c' \, r_{iso} \quad ; \quad f_{dev} = q - Mp' \left(1 - b \, Log \frac{d\, p'}{p_c'} \right) r_{dev} = 0 \tag{9}$$

where p' is the mean effective stress, q the deviatoric stress and p_c' the preconsolidation pressure. b, d and M are material parameters. In addition to the volumetric plastic strain, ε_v^p, p_c' depends on temperature T and suction s, what introduces thermo-plasticity and suction-induced plasticity (Salager et al., 2008):

$$p_c' = \begin{cases} p_{c0}' \exp\left(\beta \ \varepsilon_v^p\right) \left\{ 1 - \gamma_T \log\left[T / T_0 \right] \right\} & \text{if } s \le s_e \\ p_{c0}' \exp\left(\beta \ \varepsilon_v^p\right) \left\{ 1 - \gamma_T \log\left[T / T_0 \right] \right\} \left\{ 1 + \gamma_s \log\left[s / s_e \right] \right\} & \text{if } s \ge s_e \end{cases} \tag{10}$$

where p'_{c0} is the initial preconsolidation pressure at ambient temperature T_0 and for suction lower than the air-entry value s_e. β is the plastic compressibility modulus and γ_T and γ_s are material parameters.

r_{iso} and r_{dev} are the degree of mobilization of the isotropic and the deviatoric mechanisms and are hyperbolic functions of the plastic strain induced by the isotropic and the deviatoric mechanisms, respectively (Hujeux, 1979; Laloui & Francois, 2009). This enables a progressive evolution of the yield limit during loading and a partial release of this limit during unloading.

Water retention behaviour

In terms of water retention response, desaturation is also a yielding phenomenon. Hysteresis in water retention behaviour is modelled as a plastic process. As long as the soil is drying, suction increases, and the degree of saturation, S_r, tends to decrease mainly when the air-entry suction s_e is reached. Under re-wetting, a hysteretic phenomenon occurs, also represented by a yielding process (Figure 3). A wetting-drying cycle activates two successive yield limits in the $(S_r - s)$ plane (f_{dry} and f_{wet}, along the drying and wetting paths, respectively):

$$f_{dry} = s - s_d = 0 \quad ; \quad f_{wet} = s_d s_{hys} - s = 0 \tag{11}$$

where s_d is the drying yield limit and s_{hys} a material parameter considering the size of the water retention hysteresis. Because air-entry suction of the materials depends on temperature and dry density, sd is a function of temperature T and volumetric strain ε_v (François & Laloui, 2008) :

$$s_d = s_{d0}\left\{1 - \theta_T \log\left[T/T_0\right] - \theta_e \log\left[1-\varepsilon_v\right]\right\} \tag{12}$$

where θ_T and θ_e are material parameters describing the evolution of air-entry suction with respect to temperature and volumetric strain, respectively. If the initial state is saturated, the initial drying limit s_{d0} is equal to air-entry suction s_e and increases when suction overtakes s_e as follows:

$$s_{d0} = s_e \exp\left(-\beta_h \, \Delta S_r\right) \tag{13}$$

where β_h is the slope of the desaturation curve in the $\left(S_r - \ln s\right)$ plane (see Figure 3). The evolution of s_d with respect to T and ε_v is described by Equation (12).

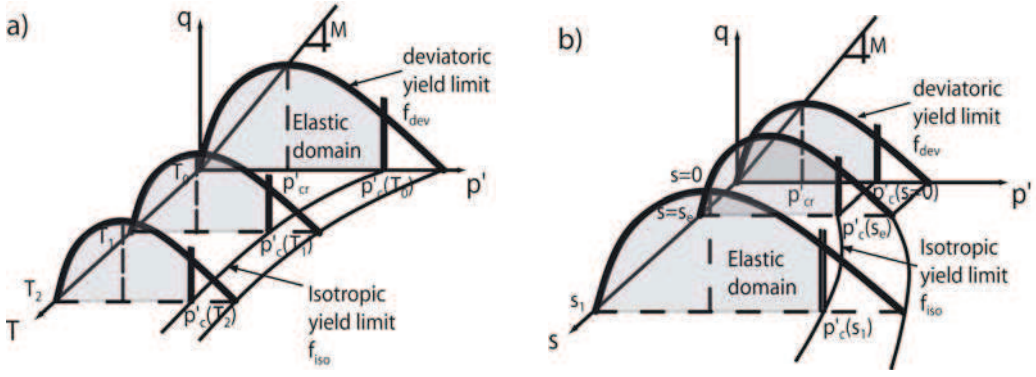

Figure 2: ACMEG-TS: Effect of (a) temperature and (b) suction on the shape of mechanical yield limits.

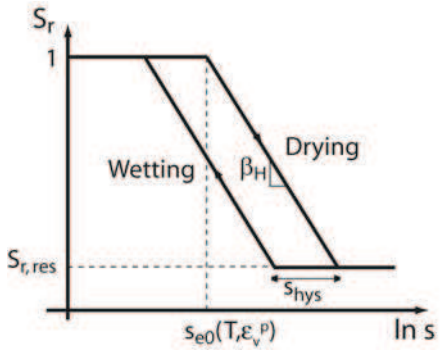

Figure 3: ACMEG-TS: Schematic representation of water retention curve modelling.

4 MATERIAL CHARACTERISTICS

FEBEX bentonite

The clay barrier was constructed with highly compacted FEBEX bentonite blocks with an initial void ratio of 0.6 and an initial water content comprised between 12.5 % and 15.5 %, corresponding to an initial suction of 110 to 130 MPa (Lloret et al., 2004). This corresponds to an initial dry density of the blocks of around 1700 kg.m^{-3}, and a degree of saturation between 35 and 45 %. The THM properties of the FEBEX bentonite have been extensively investigated over the last decade. Its mechanical behaviour under non-isothermal and unsaturated conditions has been characterised by means of several experimental programs by Villar, Lloret, Romero et al. (ENRESA, 2000; Villar, 2002; Lloret et al., 2003; Lloret et al., 2004; Villar et al., 2005).

The results of these studies have shown that, on the mechanical side of the problem, the simulation of the confined swelling behaviour of bentonite is the most important feature to reproduce. Pintado et al. (2002) performed swelling pressure tests in oedometric conditions on samples of FEBEX bentonite that were less compacted than the blocks used in the in-situ experiment. Depending upon density and suction, swelling pressures ranged from 3 to 8 MPa. Due to the difference in initial dry density between the experiment and the emplaced bentonite blocks, it has been decided to calibrate the model with a 10 MPa swelling pressure, which corresponds to the initial dry density of the blocks, i.e. 1700 kg.m^{-3}, according to the trend reported by Lloret et al. (2004).

Another important feature in the simulated scenario is the thermal response of the materials. Reference ENRESA (2000) provides the necessary information concerning the thermal expansion of compacted FEBEX bentonite. A conservative value has been chosen according to this document of 2.1×10^{-4} K^{-1} (volumetric coefficient), in order to mitigate the absence of gaps in the simulation whereas some construction gaps exist in the actual experiment.

A range of experiments and choices enabled calibration of the model with parameters defining the mechanical and water retention behaviour, as presented in Table 1. It should be noted that due to the lack of information on the shear behaviour of the material, the deviatoric mechanical parameters have been assigned with usual values for such a kind of clay.

The parameters governing the thermal and hydraulic diffusion in FEBEX bentonite are established from a review of the literature. Villar (2002) reported the saturated hydraulic conductivity as a function of the dry density. The thermal diffusion of each phase has been calibrated to reproduce the experimental evolution of the thermal diffusion of the bentonite

with respect to its degree of saturation (as reported in (Gens et al., 1998)) yielding the following parameters $(\lambda_s\ ;\ \lambda_w\ ;\ \lambda_a) = (0.7\ ;\ 2.1\ ;\ 0)\ \left[W/(m°C)\right]$. The heat capacity of the solid matrix is $c_s = 1091\ J/(kg°C)$ (Gens et al., 1998).

Table 2 reports the material parameters of FEBEX bentonite in relation to the thermal and hydraulic diffusion processes. The parameters of the water retention curve have been previously defined in Table 1.

Elastic parameters		
E_{ref}, ν, p_{ref}, n^e, β'_s	[MPa], [-], [MPa], [-], [°C^{-1}]	48, 0.3, 1, 1, 2.1×10^{-4}
Isotropic plastic parameters		
β, γ_s, γ_T, r^e_{iso}, p'_c	[-], [-], [-], [-], [-], [MPa] , [-]	10, 10, 0.2, 0.7, 2.2
Deviatoric plastic parameters		
b, d, M, g, α, a, r^e_{dev}	[-], [-], [°], [-], [-], [-], [-]	1, 1.5, 1.2, 0, 1, 0.001, 0.8
Water retention parameters		
s_{e0}, β_h, θ_T, θ_e, s_{hys}	[MPa], [-], [-], [-], [-]	4, 6.33, 0.1, 5, 0.9

Table 1: Set of FEBEX bentonite parameters for ACMEG-TS model.

Granite and other materials

The Grimsel test site has been excavated in a predominately granite and granodiorite rock. Hydraulic and mechanical properties of the Aare massif granite have been compiled in several internal reports and have been partially reported by Alonso et al. (2005) and Gens et al. (1998). The mechanical behaviour of the granite is modelled by an elastic model and is assumed to be fully saturated even under negative pore water pressure.

The material parameters of the steel of the heaters, as well as the concrete of the plug, have been chosen in the range of usual parameters for those types of material. Their mechanical behaviours have been assumed to be linear elastic. The steel is considered as impervious and the concrete plug as fully saturated. Table 2 reports the chosen parameters for the three materials.

5 FEATURES OF THE ANALYSIS OF FEBEX IN-SITU EXPERIMENT

The problem is treated under axisymmetric conditions around the y-axis, which is the axis of the test drift (Figure 4) and consequently gravity is not considered. The distance of the external boundary to the engineered barrier is the same (60 m) in both the axial and radial directions. The modelled domain is sufficiently large to avoid the undesired effects of the imposed boundary conditions in the far-field and to model the dissipation of pore water pressure during the excavation stage. The first stage of the simulation is a preliminary hydro-mechanical calculation of the excavation phase. The goal is to obtain the initial pore water pressure in the host granite, during the ventilation of the drift, and also to get realistic stresses in the host rock, while keeping the radial stress along the drift at zero. An initial isotropic total stress of 28 MPa is imposed on the granite. The water pressure is initially equal to 0.7 MPa over the whole domain, and is brought to the atmospheric pressure on the drift surface for 1000 days. Due to the phasing of construction, the bentonite, canisters and plug elements are not included in the mesh during this first stage, as they are not present during the excavation and ventilation phase. The second stage begins with the introduction of these three elements.

Thermal parameters			Bentonite	Granite	Concrete	Canister
Solid thermal conductivity	λ_s	[W/(m.°C)]	0.7	-	-	-
Water thermal conductivity	λ_w	[W/(m.°C)]	2.1	-	-	-
Air thermal conductivity	λ_a	[W/(m.°C)]	0	-	-	-
Global thermal conductivity	Γ	[W/(m.°C)]	-	3.34	1.7	-
Solid heat capacity	$c_{p,s}$	[J/(kg.°C)]	1091	-	-	-
Water heat capacity	$c_{p,w}$	[J/(kg.°C)]	4200	-	-	-
Gas heat capacity	$c_{p,a}$	[J/(kg.°C)]	1000	-	-	-
Global heat capacity	C_p	[J/(kg.°C)]	-	1000	750	-
Liquid thermal expansion coefficient	β'_w	[°C^{-1}]	4 10^{-4}	4 10^{-4}	4 10^{-4}	-
Solid thermal expansion coefficient	β'_s	[°C^{-1}]	2.1 10^{-4}	2.5 10^{-5}	1 10^{-5}	2.5 10^{-5}
Hydraulic parameters						
Intrinsic water permeability	$k_{w0,sat}$	[m^2]	4 10^{-21}	4.5 10^{-19}	1 10^{-19}	
Kozeny-Carman coefficient 1	$EXPM$	[-]	6.5	0	0	-
Kozeny-Carman coefficient 2	$EXPN$	[-]	6.5	0	0	-
Relative permeability coefficient	$CKW1$	[-]	2.9	-	-	-
Volumetric parameters						
Initial porosity	n_0	[-]	0.4	0.01	0.15	0
Tortuosity	τ	[-]	0.5	0.6	0.6	
Solid specific mass	ρ_s	[kg/m^3]	2700	2660	2500	7800
Water specific mass	ρ_w	[kg/m^3]	1000	1000	1000	-
Air specific mass	ρ_a	[kg/m^3]	1.18	-	-	-
Liquid compressibility	$1/\chi_w$	[Pa^{-1}]	3.33 10^{-10}	3.33 10^{-10}	3.33 10^{-10}	-
Mechanical parameters						
Young elastic modulus	E	[MPa]	See Table 1	5000	3000	20000
Poisson ratio	υ	[-]		0.35	0.2	0.3

Table 2: Parameters of the various materials involved in the simulation of the FEBEX in-situ experiment.

In the bentonite, suction of 114 MPa is considered as the initial hydraulic condition. The external total stress is initially equal to zero at the beginning of the second stage. This corresponds to a generalised mean effective stress of 53.9 MPa, equal to the product $S_r \times s$ at the initial temperature (Equation 7). The bentonite is assumed to be normally consolidated ($p'_{c0} = 2.2MPa$; $\gamma_s = 10$; $s_0 = 114MPa$). The canister and the concrete plug are also under zero stress. The air pressure has been fixed to atmospheric pressure over the entire unsaturated domain.

In the computation, the construction gap, evaluated as 5.53 % of the emplacement volume (Alonso et al., 2005), has not been considered. This implies that the swelling pressure predicted by the numerical simulations will be overestimated. This swelling caused by progressive wetting starts with this second stage and lasts four months before heating begins.

In the experiment, the temperature ramp was imposed with a controlled power (1200 W per heater for 20 days and 2000 W per heater over the following 33 days until reaching the desired temperature of 100 °C). The same scheme has been reproduced in the simulation. Due to the insulating air gaps, the power applied in the simulation is only 85 % of the real power, with the same ramp up, and the centre of the heaters reaches 100 °C at the correct time. The temperature on all heater nodes is then kept constant for the rest of the simulation. The simulation has been performed on the total time of operation (i.e. 5 years). For all subsequent graphs, zero-time corresponds to the start of the heating (February 27th 1997).

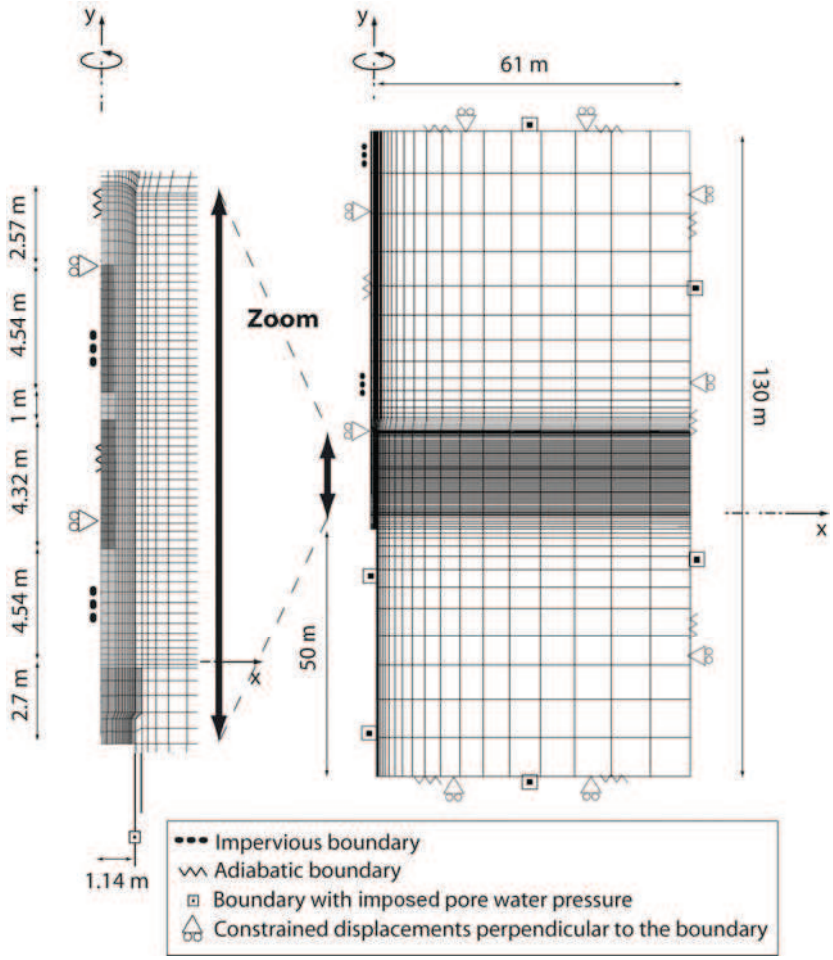

Figure 4: Finite element mesh used in the simulation of the in-situ FEBEX experiment. The y axis is the axis of symmetry of revolution (y=0 corresponds to the bentonite/plug contact).

6 RESULTS OF SIMULATION COMPARED WITH MEASUREMENTS

Figure 5 to Figure 7 compare numerical results to experimental measurements at various locations. The indicated letters in figures correspond to sections, and are shown in Figure 1. The associated number corresponds to the radial rank of the node: 0 is for the centre of the tunnel, 2 for the heater radius, 10 for the frontier between the bentonite and granite, and higher numbers are located in the granite. The nodes are chosen for their proximity to actual sensors.

Figure 5 presents the evolution of temperature over time in three sections of the engineered barrier and in one borehole in the rock mass. Points F2-2 and I-2 being on the heater surface, their temperatures remain constant in the last phase, but there is a clear difference in their temperature. In section I, we observe a steady thermal gradient of about 60 °C across 66 cm after 500 days (from 95°C at x = 0.48 m to 45 °C at x = 1.14 m). On the other hand, far away from the heater (section B2, Figure 5 left, and boreholes K1 and K2, Figure 5 right), the temperature continuously increases, even after five years of heating. The results of the simulation show good agreement with in-situ measurements.

The relative humidity in the bentonite is obtained in the simulation from the temperature and suction through Kelvin's law. Figure 6 displays the comparison between the measured

and the computed values in two different sections of the engineered barrier. The simulated processes are also presented before zero-time, so that one can see why both the zero-time experimental and simulated fields are not uniform. The simulation starts from a homogeneous relative humidity field of about 40% (corresponding to s = 114 MPa and T = 12°C), and in the simulation wetting starts immediately at the frontier between the granite and bentonite, because of the water flow from the saturated granite to the unsaturated bentonite. The sensor measurements show an initial gradient of relative humidity in each section, which is closely matched by the simulations. Close to the heater, the bentonite is dried due to thermally-induced water evaporation (Figure 6, left, point E1-2). Vapour arising from that drying diffuses outwards and condensates in the cooler region, causing accelerated wetting of the bentonite in the central part. In addition the more heated bentonite initially dilates and pressurises the more central one, therefore increasing the relative humidity at the centre. This effect is clearly visible in the wetting rate at point F2-6 (Figure 6, left), before and after the heating. A rapid increase from 40 to 60 % is observed, while the trend before heating indicated a very slow increase. Close to the granite the effect of temperature on the resaturation of bentonite is not so obvious, as its evolution does not seem to be affected by heating at time t_0 (Point C-9).

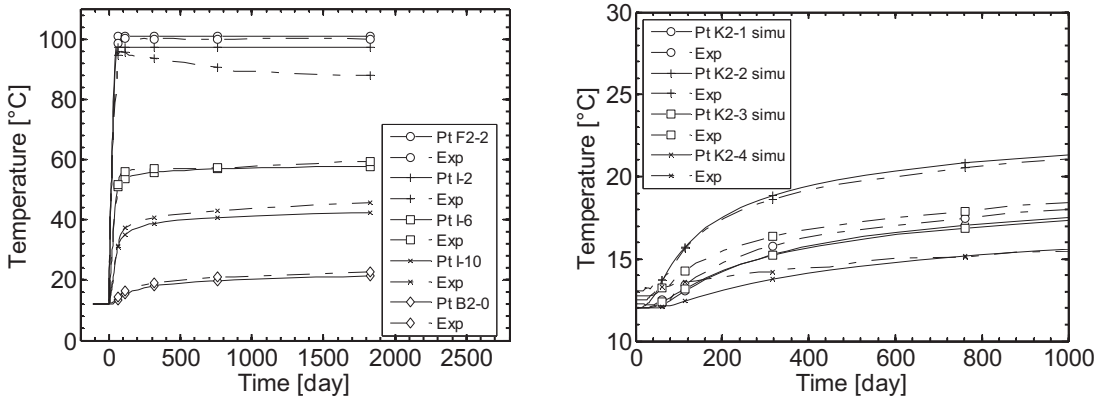

Figure 5: Variation of temperature with time at five points (distributed in three sections) of the engineered barrier, and in one borehole in the host rock. Comparison between numerical simulation (full lines) and experimental measurements (dashed lines).

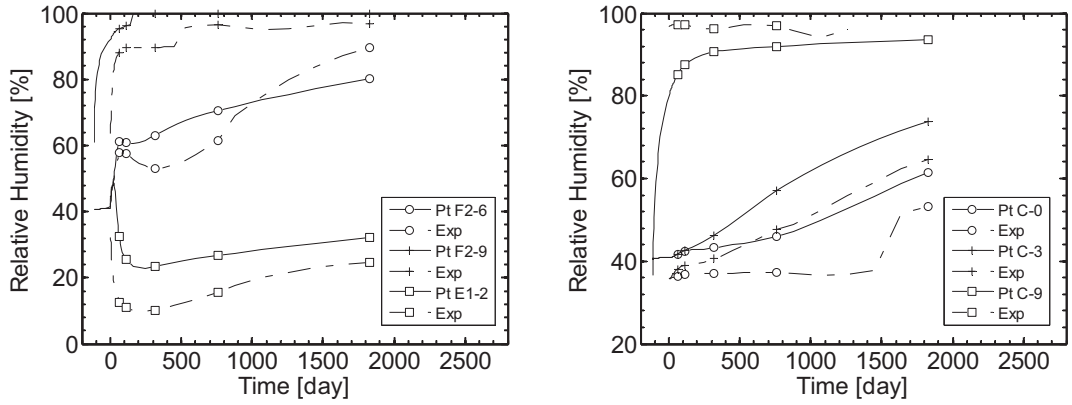

Figure 6: Variation of relative humidity with time at nine points distributed between heater and host rock (left graph) and in a section far from the heaters (right graph). Comparison between numerical predictions (full lines) and experimental measurements (dashed lines).

Figure 7 (left) displays the evolution of total mean stress along a borehole in section G, at radial distances of 2.2, 3.3 and 7.1 m. The simulation shows relatively good agreement with the sensors, given the mechanical assumptions made in the simulation (no construction gap allowing some free swelling of the bentonite). The most important difference comes from the peak in net mean stress that is observed experimentally in the most central sensor. This peak is only observed in the radial component of the stresses in the simulation. This can be more clearly seen in Figure 7 (right), which represents the radial displacements in a radial borehole, reset to zero at zero-time. The peak in displacement induced by the peak in the swelling pressure of bentonite is clearly visible in both the simulation and experiment, and was not observed in previous studies. Although its magnitude is greater than the experimental measurement, this is a very interesting feature of this model, which clearly reproduces the trend observed in reality.

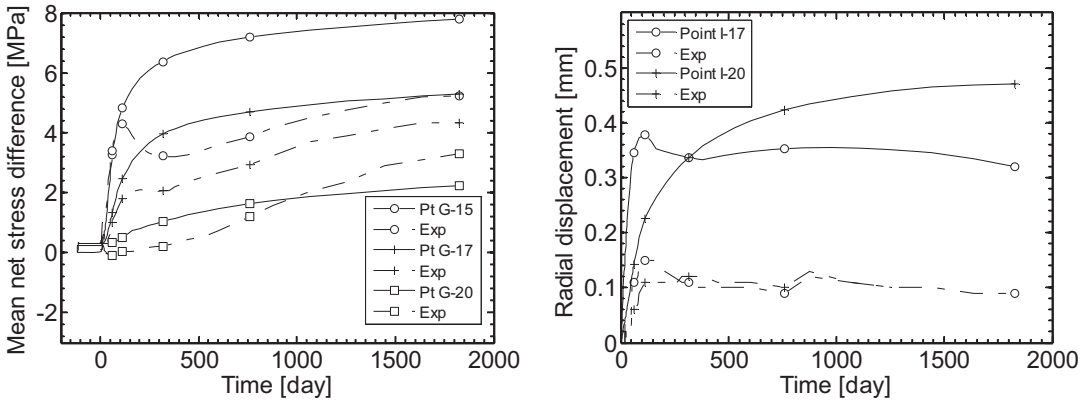

Figure 7: (left) Variation with time of mean net stress in a radial borehole in the middle section of the experiment, at radial distances 2.2, 3.3 and 7.1 m. The reference state is that of granite after the excavation of the drift. Comparison between numerical predictions (full lines) and experimental measurements (dashed lines). (right) Variation with time of radial displacement (outwards positive) in a radial borehole in section I. Comparison between numerical predictions (full lines) and experimental measurements (dashed lines).

7 CONCLUSIONS

Facing the need to analyse and predict the long-term behaviour of underground disposal facilities for nuclear waste, the primary aim of this numerical analysis is to provide a means for assessing and understanding the thermal, hydraulic and mechanical responses of bentonite and the surrounding rock involved in a multi-barrier system. The interpretation of the THM processes requires comprehensive constitutive models and numerical tools in order to incorporate most of the material behavioural features.

The FEBEX in-situ test is a near-to-real experiment of nuclear waste disposal in a granitic formation. The THM behaviour of the buffer material (made of FEBEX bentonite) and the surrounding host rock (granite), encountering many complex and interconnected THM phenomena, has been modelled by means of finite element simulations.

The parameters of the thermo-plastic constitutive model used for saturated and unsaturated materials, named ACMEG-TS, have been defined after a thorough review of the literature and the choice of the confined swelling pressure as the main feature.

The features of the numerical analysis have been presented. Subsequently, the obtained results have been compared with the available sensors measurements in both the engineered barrier and the granite. The results of the simulations show good agreement with the

experiment. The confined swelling behaviour of highly compacted bentonite is well reproduced by the constitutive model, in terms of both magnitude and behaviour. It is an important feature of the ACMEG-TS model, and is directly obtained from the introduction of a wetting collapse mechanism in the framework of generalised effective stress.

The use of a performant finite element code, coupled with an advanced thermo-plastic constitutive model using an unsaturated formalism, significantly advances the knowledge of the highly coupled processes occurring in a clayey formation, initially unsaturated, in the near field of a heat-emitting radioactive waste.

ACKNOWLEDGMENTS

The authors would like to acknowledge NAGRA for funding and supporting this research, and also wish to thank Prof. R. Charlier and Dr. F. Collin for their collaboration and their advice regarding the implementation of the model in the LAGAMINE finite element code.

REFERENCES

Alonso, E.E., Alcoverro, J., Coste, F., Malinsky, L., Merrien-Soukatchoff, V., Kadiri, I., Nowak, T., Shao, H., Nguyen, T.S., Selvadurai, A.P.S., Armand, G., Sobolik, S.R., Itamura, M., Stone, C.M., Webb, S.W., Rejeb, A., Tijani, M., Maouche, Z., Kobayashi, A., Kurikami, H., Ito, A., Sugita, Y., Chijimatsu, M., Börgesson, L., Hernelind, J., Rutqvist, J., Tsang, C.F. & Jussila, P. (2005). "The FEBEX benchmark test: case definition and comparison of modelling approaches." Int. J. Rock Mech. Min. Sc. Vol. 42(5-6), 611-638.

Charlier, R., Radu, J.-P. & Collin, F. (2001). "Numerical modelling of coupled transient phenomena." Rev. Fr. Génie Civ.

Collin, F. (2003). "Couplages thermo-hydro-mécaniques dans les sols et les roches tendres partiellement saturés." Department ArGEnCo. Liège, Belgium, Université de Liège. PhD.

Collin, F., Li, X.L., Radu, J.P. & Charlier, R. (2002). "Thermo-hydro-mechanical coupling in clay barriers." Eng. Geol. Vol. 64(2-3), 179-193.

ENRESA (2000). "Febex Project: Full-scale engineered barriers experiment for a deep geological repository for high level radioactive waste in crystalline host rock." Publicación técnica. Madrid, Spain, ENRESA**:** 354.

François, B. & Laloui, L. (2008). "ACMEG-TS: A constitutive model for unsaturated soils under non-isothermal conditions." Int. J. Numer. Anal. Meth. Vol. 32(16), 1955-1988.

Gens, A., Garcia-Molina, A.J., Olivella, S., Alonso, E.E. & Huertas, F. (1998). "Analysis of a full scale in situ test simulating repository conditions." Int. J. Numer. Anal. Meth. Vol. 22(7), 515-548.

Gens, A., Sánchez, M., Guimarães, L.d.N., Alonso, E.E., Lloret, A., Olivella, S. & Villar, M.V. (2009). "A full-scale in situ heating test for high-level nuclear waste disposal: observations, analysis and interpretation." Géotechnique Vol. 59(4), 377-399.

Hujeux, J.-C. (1979). "Calcul numérique de problèmes de consolidation élastoplastique." Paris, France, Ecole Centrale. PhD.

Laloui, L. & Francois, B. (2009). "ACMEG-T: Soil Thermoplasticity Model." J. Eng. Mech. Vol. 135(9), 932-944.

Laloui, L., François, B., Nuth, M., Péron, H. & Koliji, A. (2008). "A thermo-hydro-mechanical stress-strain framework for modeling the performance of clay barriers in deep geological repositories for radioactive waste." 1st European Conf. on Unsaturated Soils. Durham, UK.

Lloret, A., Romero, E. & Villar, M.V. (2004). "FEBEX II Project: Final report on thermo-hydro-mechanical laboratory tests." Publicación técnica. Madrid, Spain, ENRESA**:** 165.

Lloret, A., Villar, M.V., Sánchez, M., Gens, A., Pintado, X. & Alonso, E.E. (2003). "Mechanical behaviour of heavily compacted bentonite under high suction changes." Géotechnique Vol. 53(1), 27-40.

Nuth, M. & Laloui, L. (2008). "Effective stress concept in unsaturated soils: Clarification and validation of a unified framework." Int. J. Numer. Anal. Meth. Vol. 32(7), 771-801.

Pintado, X., Ledesma, A. & Lloret, A. (2002). "Backanalysis of thermohydraulic bentonite properties from laboratory tests." Eng. Geol. Vol. 64(2-3), 91-115.

Salager, S., François, B., El Youssoufi, S., Laloui, L. & Saix, C. (2008). "Experimental investigations on temperature and suction effects on compressibility and pre-consolidation pressure of a sandy silt." Soils Found. Vol. 48(4), 453-466.

Schrefler, B.A. (1984). "The finite element method in soil consolidation (with applications to surface subsidence)." Swansea, UK, University College. PhD.

Villar, M.V. (2002). "Thermo-hydro-mechanical characterisation of a bentonite from Cabo de Gata: A study applied to the use of bentonite as sealing material in high level radioactive waste repositories." Publicación técnica. Madrid, Spain, ENRESA.

Villar, M.V., García-Siñeriz, J.L., Bárcena, I. & Lloret, A. (2005). "State of the bentonite barrier after five years operation of an in situ test simulating a high level radioactive waste repository." Eng. Geol. Vol. 80(3-4), 175-198.